

# Comparison of Hot-Film Probe and Optical Techniques for Sensing Shock Motion

Frederick W. Roos\* and Thomas J. Bogart†  
*McDonnell Douglas Corporation, St. Louis, Mo.*

Two independent shock position sensing techniques have been compared experimentally. One technique utilizes a hot-film probe controlled by a constant-temperature anemometer unit; the other method is strictly optical, employing a shadowgraph system and a line-scan television camera. The techniques were employed simultaneously in a two-dimensional transonic diffuser flow with a shock wave. For the case of natural, random shock motion, the two systems produced similar results throughout the range of Mach numbers studied, in terms of both the amplitude and frequency content of the data signals. Tests were also conducted in which the shock wave was forced into periodic oscillation at several frequencies; excellent agreement was obtained between the average waveforms of the shock motion data signals produced by the two techniques. Each technique possesses some definite advantages over the other; relative merits and applications of the two methods are discussed.

## Introduction

TWO independent techniques have been developed recently for generating a real-time analog signal that represents the streamwise position of a shock wave in a transonic flow. One of these techniques uses a hot-film probe that is operated by a conventional constant-temperature anemometer set,<sup>1</sup> while the other method is strictly optical, employing a shadowgraph light source and optics in conjunction with a line-scan television-type camera.<sup>2</sup> The hot-film probe technique was developed for use in wind-tunnel studies of shock wave motion in the flowfield of a transonic airfoil during buffeting, a situation in which it was initially believed that spanwise nonuniformity might exist. The optical technique, on the other hand, was applied to a study of shock wave unsteadiness in a transonic diffuser flow that was known to be essentially two dimensional. Unlike the hot-film probe technique, which involves only a local measurement and hence is applicable in three-dimensional flowfields, the optical method is inherently a two-dimensional technique.

An opportunity recently arose for the direct comparison of the two shock motion monitoring techniques in a two-dimensional transonic channel flow that included a shock wave. This paper presents the results of that comparative evaluation.

## Hot-Film Probe Technique

The hot-film probe technique<sup>1</sup> makes use of a standard constant-temperature anemometer circuit to heat a metal film on the surface of an aerodynamically shaped, cylindrical quartz rod that is aligned with the mean flow. When the probe is piercing a shock wave, the rates of heat transfer from the heated film are different upstream and downstream of the shock. Consequently, the heating current required to maintain the metal film at a constant overall temperature (i.e., constant resistance) varies with the position of the shock along the probe axis. While the hot-film shock position sensing probe technique has been employed successfully in a study of

transonic airfoil buffeting,<sup>3</sup> the small probes originally used did not have sufficient sensor length to accommodate the full range of shock wave excursions for all conditions of interest. To remedy this shortcoming, a family of larger probes has since been developed and tested. These probes were all built according to the same split, heated metal film principle as the original hot-film probes<sup>1</sup>; configurations of the various new probes are shown in Fig. 1. Characteristics of the probes are given in Table 1. Whereas the original probes were capable of monitoring shock wave motion over a streamwise distance of only about 0.76 cm, the largest of the new probes has a sensitive length of 5.0 cm.

## Optical Technique

The optical shock location detecting system uses shadowgraph optics and a line-scan television camera (Fig. 2). The camera contains a linear array of 256 photodiodes (pixels) onto which an image of the shadow cast by the shock wave is focused. The pixels are scanned at a rate of 4 kHz. Simple electronics allow the location of the shock to be determined by sensing the pixels onto which the shadow is cast. A detailed description of the system appears elsewhere.<sup>2</sup> The camera is equipped with a 200-mm zoom lens, and, with the physical arrangement used, total shock excursions of up to 8 cm can be tracked, which corresponds to a spatial resolution of approximately 0.3 mm per pixel. Natural oscillations of the shock wave in this diffuser occur at frequencies below 250 Hz, so the camera scan rate of 4 kHz is sufficient to define accurately the shock wave motion.

The pulse-width modulation decoding circuit has been modified slightly from its original form<sup>2</sup>; the area within the dashed box in the circuit diagram (Fig. 3) represents the modification. The signal from the scan clock is inverted and sent to the "B" input of the monostable multivibrator. This

Table 1 Hot-film probe physical characteristics

Model	Diameter, $D$ , mm	Sensor length, $L_s$ , mm	Tip length, $L$ , mm	Room temperature resistance, $\Omega$
A-1	1.52	50.6	59.2	17.50
A-2	1.52	39.1	47.7	12.85
B-1	1.02	31.5	37.6	14.44
B-2	1.02	25.4	31.0	10.77
B-3	0.76	19.0	23.1	11.90

Presented as Paper 81-0157 at the AIAA 19th Aerospace Sciences Meeting, St. Louis, Mo., Jan. 12-15, 1981; submitted Feb. 23, 1981; revision received Nov. 16, 1981. Copyright © American Institute of Aeronautics and Astronautics, Inc., 1981. All rights reserved.

\*Scientist, McDonnell Douglas Research Laboratories. Associate Fellow AIAA.

†Research Scientist, McDonnell Douglas Research Laboratories. Member AIAA.

change ensures proper updating of the integrator should a "dropout" occur, that is, should the pixel array be scanned without the shock being detected.

### Experimental Setup

The new hot-film shock position sensing probes were calibrated and compared with the optical system in a two-

dimensional diffuser model (Fig. 4) that was designed specifically for studies of shock wave motion in transonic diffuser flow.<sup>4</sup> The model has an exit-to-throat area ratio of 1.5 and an exit width-to-height aspect ratio of 2.46. The latter, together with removal of side- and bottom-wall boundary layers through a series of suction slots, helps to ensure two-dimensionality of the flow within the diffuser. For the present study, the shock Mach number  $M_{sh}$  was varied between 1.23 and 1.36. Although limited, this range of  $M_{sh}$  values actually encompasses the shock strengths usually associated with normal shocks in transonic flows, particularly those over airfoils.

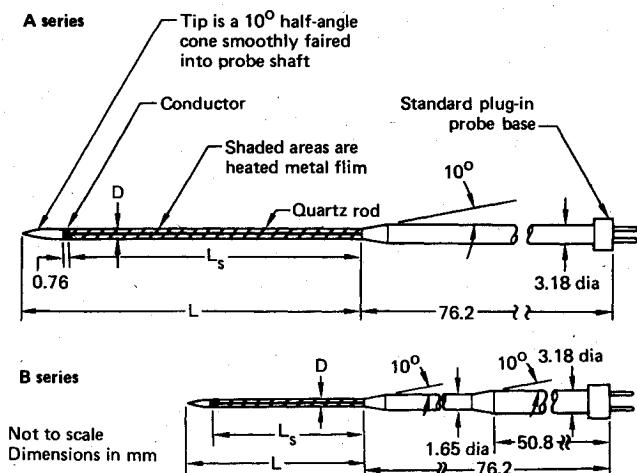


Fig. 1 Hot-film shock position sensing probe designs.

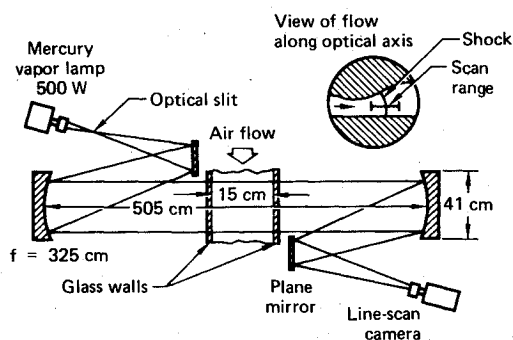


Fig. 2 Layout of optical shock location detection system.

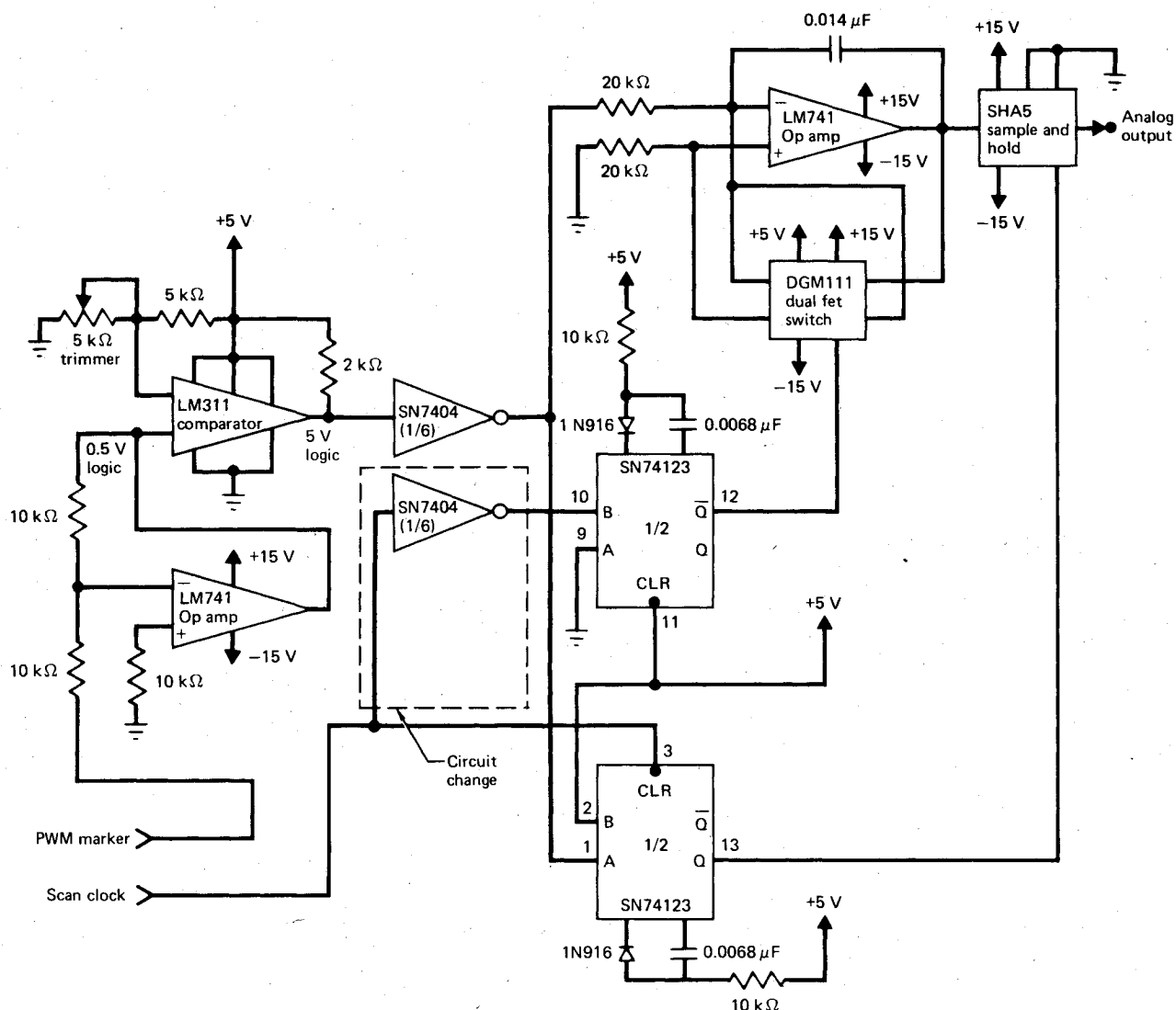
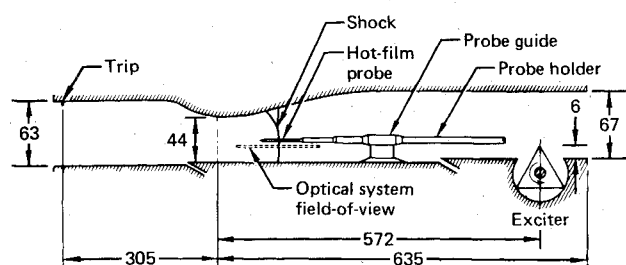


Fig. 3 Revised pulse-width modulation decoding circuit.



Dimensions in mm  
Vertical dimensions and slot sizes enlarged.

Fig. 4 Two-dimensional transonic diffuser model used for shock motion detection comparison tests.

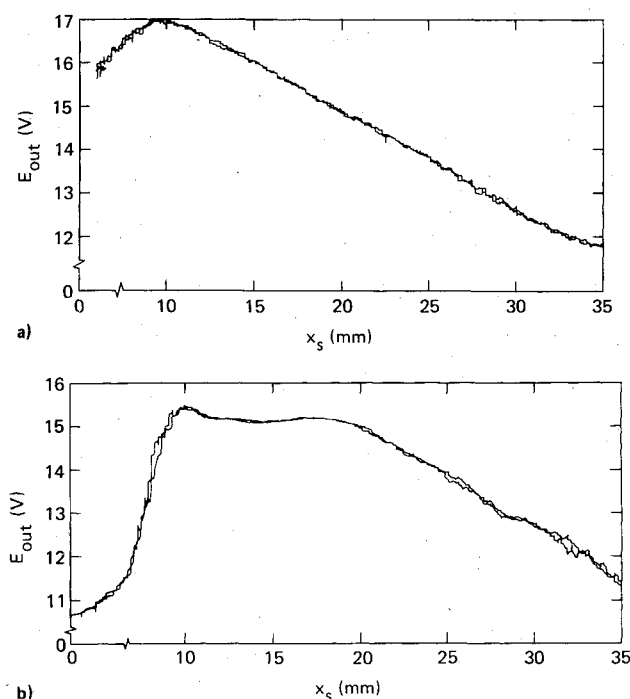


Fig. 5 Typical hot-film shock probe calibrations (probe B-1): a) overheat ratio = 1.14, and b) overheat ratio = 1.02.

The side walls of the diffuser are fitted with optical quality glass windows, which extend from the throat to the end of the divergent section of the model. These windows are flat to within 3 wavelengths/m and are parallel to within 3 arc-sec. They allow optical access for schlieren, shadowgraph, and laser velocimeter measurements. In particular, they permit utilization of the optical shock location detecting system, which was originally developed for use with this diffuser model.

Upstream-propagating pressure waves are generated by rotation of the triangular exciter at the exit end of the diffuser, which in effect produces periodic modulation of the diffuser exit area. The rotation rate of the exciter is continuously variable up to 110 Hz, which corresponds to pressure fluctuations of up to 330 Hz. The depth to which the exciter penetrates the flow is continuously variable up to a maximum of 1.3 cm, for an area modulation of up to 19%. For most of the present work, the exciter depth was 0.6 cm. When not in use, the exciter was locked so that one face was flush with the diffuser bottom wall.

The field of view of the optical shock-detection system is indicated in Fig. 4, as is the location of a typical shock wave ( $M_{sh} = 1.36$ ) in the diffuser. The hot-film probe is fitted into a holder, which in turn passes through a guide and extends beyond the diffuser exit. A positioning mechanism located

beyond the end of the diffuser moves the shock probe axially and provides an indication of its position.

## Results

### Calibration

Probes were calibrated by traversing them slowly through the shock while recording shock position relative to the probe ( $x_s$ ) and the constant-temperature anemometer output voltage ( $E_{out}$ ) on the two axes of an X-Y plotter. It was necessary to filter the anemometer output with a low cutoff frequency in order to minimize "jitter" resulting from the small-amplitude natural oscillations of the shock in the diffuser. Unfortunately, the long time constant associated with the low filter frequency required that the calibration be done slowly, which led to some difficulties with the probe-positioning mechanism and with maintaining constant diffuser flow conditions. Obtaining an accurate probe calibration proved to be the most serious difficulty encountered in using the hot-film shock probe.

Linearity of the shock probe output is a strong function of the probe overheat ratio, as Fig. 5 indicates. Overheat ratio (OR) is defined as the ratio of the overall resistance of the heated probe to the resistance of the unheated probe. The linearity of the calibration at the higher overheat ratio (1.14) is clearly evident in Fig. 5a, while Fig. 5b reveals substantial nonlinearity at low overheat (1.02). The latter overheat ratio is obviously too low for effective use of this probe. This sort of nonlinearity at low overheat results from the combined effects of several secondary influences on probe heat transfer, such as different adiabatic wall temperatures upstream and downstream of the shock, or physical irregularities in the probe; these effects are most significant when the difference between the probe and flow temperatures is small. In general, a probe overheat ratio of 1.05 seemed to be about the minimum necessary to produce an acceptably linear calibration, especially for the larger probes. Each probe had an optimum overheat ratio, i.e., an overheat ratio that produced the most linear calibration. Optimum overheat ratios ranged from 1.05 to 1.15. Probe sensitivity was determined from the slope of the straight line that best fit the nearly linear portion of the calibration curve. Figure 6 shows how the sensitivity of typical probes varies with overheat; the evident square-root relationship is in agreement with the simple probe theory outlined in Ref. 1. Probe sensitivities are lower at the higher shock Mach number, although this probably does not represent a Mach number effect, since Mach number, Reynolds number, and local temperature and pressure vary together in this diffuser flow.

The optical shock position sensing system was calibrated with no flow. A vertical rod was placed in the shadowgraph light beam at regularly spaced intervals within the field of view of the line-scan camera, simulating the shadow cast by a shock wave. The output of the system was found to be linear with respect to the shadow location, the degree of linearity depending on the quality and alignment of the optical elements.

A dynamic calibration of the optical system was also conducted. A rapidly rotating vane was placed in the field of view of the line-scan camera, casting a shadow with a periodically moving edge over the pixel array. The fraction of the pixel array covered by the moving shadow edge was varied, as was the frequency of the vane rotation, in order to determine if the response of the system is limited by dynamic errors.<sup>2</sup> System performance was expected to be degraded with increasing shadow speed. The response of the optical shock position sensing system was found to be flat to the 400-Hz testing limit, up to the 75% limit of pixel coverage. Experimentally, frequencies of up to 330 Hz and shock motions of up to 1.4-cm rms (4.0 cm peak-to-peak) corresponding to 50% coverage of the pixels were encountered. Thus the response of this system was more than adequate.

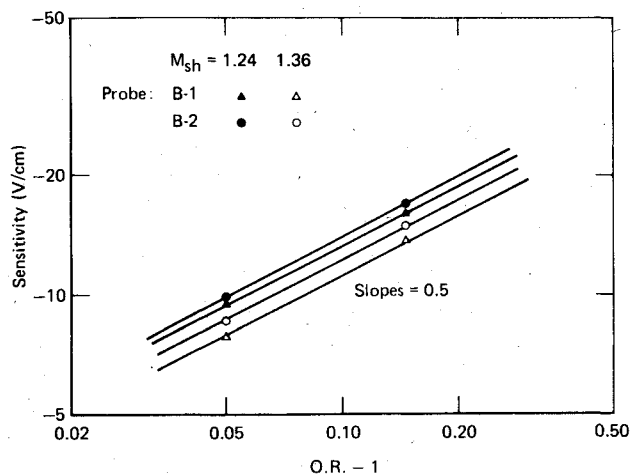


Fig. 6 Variation of probe sensitivity with overheat ratio for typical hot-film shock probes.

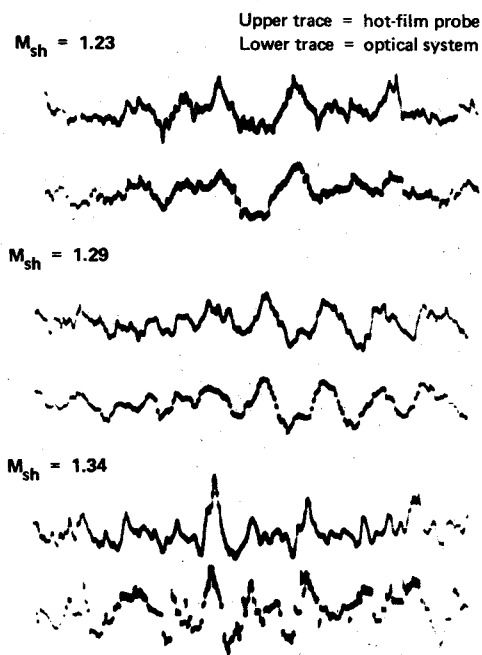


Fig. 7 Comparison of shock motion signals for several test conditions.

#### Comparison of Techniques

Initial comparison testing of the two shock position sensing systems involved the simultaneous use of both systems to monitor the natural (unexcited) random oscillations of the shock wave in the diffuser model for several different shock Mach numbers. Output signals from both systems were FM tape-recorded for later statistical processing; minimum record length in all cases was 30 s. Raw shock-motion signals from the two systems showed close agreement, as the comparisons in Fig. 7 demonstrate. Clearly the two independent techniques are responding to the same phenomenon, and the significant details of the shock motion about its mean position are tracked properly by both systems. Following filtering to eliminate effects of possible temperature or Mach number drifting, the shock displacement signals were root-mean-square processed. The resulting rms amplitudes,  $x'_s$  (Fig. 8), indicate that the agreement shown by the two techniques is quantitative as well as qualitative. Optical system results are reproducible to within  $\pm 5\%$  and, therefore, are taken to be definitive. While the shock probe data show some scatter

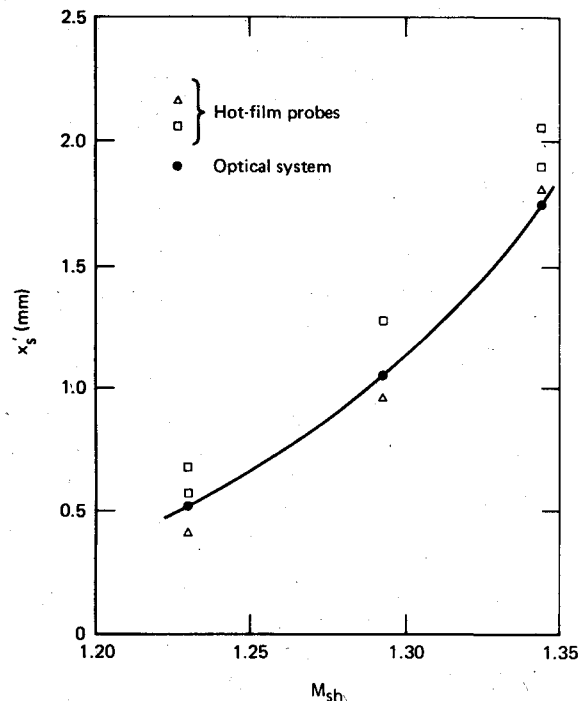


Fig. 8 Indicated rms shock displacement as a function of shock Mach number.

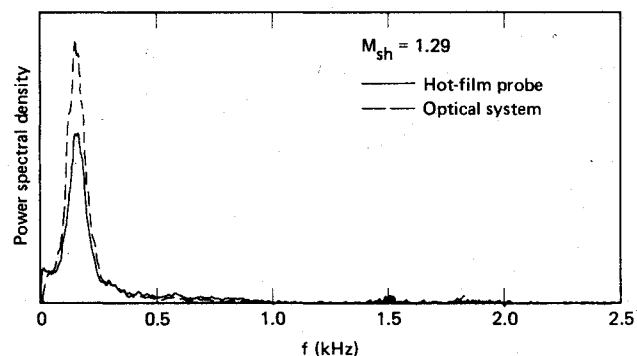


Fig. 9 Comparison of shock motion power spectra for a single-frequency case.

relative to the optical system points, the amplitude levels are reasonably well defined by the hot-film probe, and the trends are followed correctly. The scatter that appears in the hot-film probe results is believed to be connected with the difficulties encountered in precisely determining the probe sensitivities.

Frequency content of the shock motion signals produced by the two systems was established through spectral analysis. The interest here was in comparison of spectral shapes, and consequently no effort was made to compare power spectra quantitatively. Nevertheless, care was taken to ensure statistically valid results (for example, normalized standard error of the power spectral densities did not exceed 5%). At the higher shock Mach number, the shock motion power spectrum shows a single pronounced peak at the natural frequency of the shock oscillation. Figure 9 shows that both the optical system and the hot-film probe method identified the same spectral peak for such a single frequency case. At the lower shock Mach numbers (e.g.,  $M_{sh} = 1.23$ ), the shock motion is more complex; the shock motion spectrum becomes double peaked, indicating two naturally excited modes of oscillation. Shock oscillation power spectra for this case are compared in Fig. 10; both shock detection systems again correctly identify the frequency content of the shock wave motion. The spectra in Fig. 10 were not plotted to a common

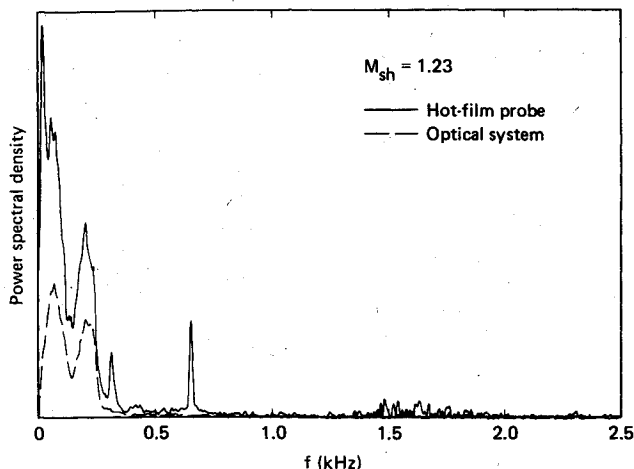


Fig. 10 Comparison of shock motion power spectra for a case of bimodal shock oscillation.

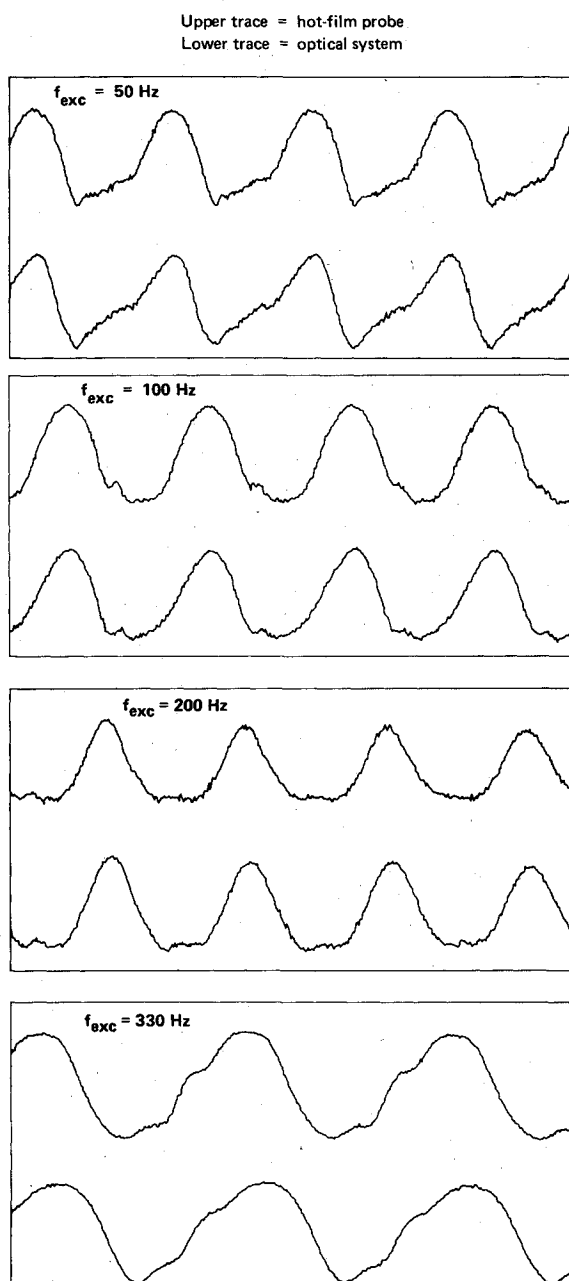


Fig. 11 Signal averaged shock motion waveforms for forced shock oscillations.

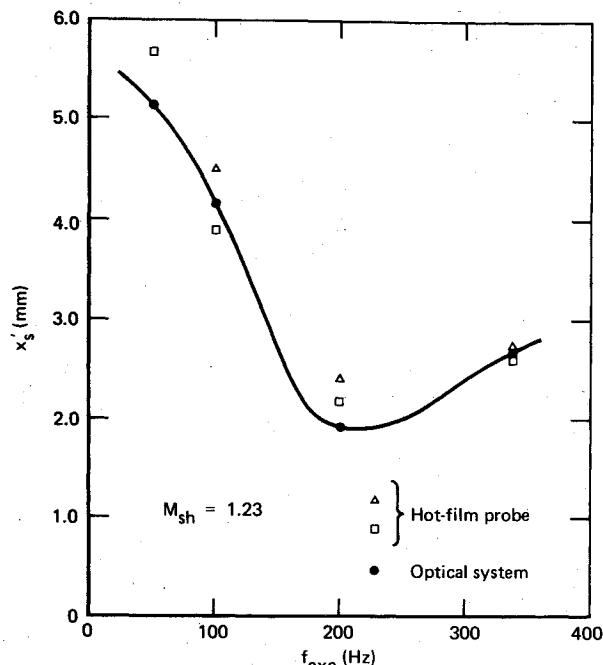


Fig. 12 Root-mean-square shock displacement amplitude vs forced oscillation frequency.

vertical scale since only the peak frequencies were of interest. Sharp peaks appearing in the shock probe data at frequencies of approximately 300 and 600 Hz resulted from mechanical vibrations of the probe and probe holder and not from any aspect of the flow or shock wave movement. The source of the peak in the hot-film probe spectrum at low frequency ( $f \rightarrow 0$ ) has not been established definitely, but is believed to be connected with low-frequency unsteadiness of the temperature or density of the flow in the diffuser, either of which would affect the heat transfer from the hot-film probe without necessarily causing movement of the shock wave. A test performed at this same flow condition but with the hot-film probe not penetrating the shock wave yielded a probe signal power spectrum that included the low-frequency peak (but not the two shock motion peaks). Peaks also appeared at the previously mentioned mechanical vibration frequencies of the probe and holder. The low-frequency peak was present in all hot-film probe spectra (for example, it is slightly indicated in Fig. 9), but appeared prominently only in the  $M_{sh} = 1.23$  spectra because of the lower signal level at that shock Mach number (recall the rms level variation shown in Fig. 8).

To further evaluate the frequency-response characteristics of the two shock motion detection systems, a test series was run in which the rotating exciter at the diffuser exit was used to drive the shock wave into periodic oscillation. Because the natural flow unsteadiness that was responsible for the unexcited shock oscillations was still present in the excited shock cases, the shock motion in these cases was actually a superposition of the shock responses to the two inputs. Signal averaging (also called signal enhancement) was employed to eliminate the randomly occurring shock movements from the data. This process amounts to ensemble averaging many repetitions of the forced excitation event, using a digitized form of the shock motion signal as input to a multichannel summer that was repetitively triggered by a timing signal from the rotating exciter. Because the naturally occurring, random shock oscillations are unrelated statistically to the periodic phenomenon, the random contribution averages to zero. Shock oscillation signals that have been processed by the signal averaging technique are presented in Fig. 11 for four excitation frequencies (amplitude scales are not the same for both systems). Root-mean-square amplitudes for these excited motion cases are plotted in Fig. 12; the greatest amplitudes

occur at the lowest frequency. The waveforms produced by the two shock sensing systems are similar at all frequencies. Even the small-scale features of the periodic shock oscillations appear to have been resolved by both systems. Differences that can be detected in the wave shapes in Fig. 11 are primarily the result of the incomplete linearity of the hot-film probe system; correspondingly, the most evident distortion appears in the 50-Hz case where the shock oscillation amplitude is greatest. As before, the amplitude results (Fig. 12) are in reasonably close agreement. The hot-film probe data again show some scatter but clearly identify the correct variation as a function of excitation frequency. Imprecision of the probe calibration and nonlinearity of the probe system output are responsible for the scatter that does exist in the rms data.

### Discussion

Both shock position detection techniques described and compared here satisfactorily perform their intended function, which is to produce a real-time analog signal that represents the streamwise position of a shock wave in a transonic flow, so that movements of the shock can be correlated directly with other sensible variations in the flow. The excellent overall agreement between the hot-film shock position sensing probe and the optical shock location detection techniques validates the utility of these completely independent approaches for measuring time-varying shock location. Each of the techniques has advantages and areas of application. In a strictly two-dimensional flowfield, the optical system is superior, for several reasons. Its output is truly linear, and it can be statically and dynamically calibrated simply, without flow, since it operates on a shadow in a parallel light beam. Furthermore, the measurement definitely responds to shock location alone; no interpretation or theory is necessary, as is the case with the hot-film probe (which actually measures heat transfer). Finally, the optical technique has the added advantage of being nonintrusive, whereas the hot-film probe must be inserted into the shock wave being studied. On the other hand, the hot-film probe is a simple, inexpensive device,

assuming that the constant-temperature anemometer set needed to operate the probe is available. Although it may require more care to be used successfully, the hot-film probe technique is capable of producing useful results, as this comparative evaluation has demonstrated. The greatest advantage of the hot-film probe technique is its ability to make shock motion measurements in three-dimensional flowfields, in which the inherently two-dimensional optical technique cannot be used.

### Conclusions

Two independent shock position sensing techniques, one optical and the other based on a hot-film probe, have been compared directly in a transonic diffuser flow. Results of the comparison have indicated that both systems satisfactorily produce analog output signals that contain the proper amplitude and frequency characteristics of the shock wave motions they are intended to monitor. In strictly two-dimensional flow, the optical system produces somewhat more accurate results; however, only the hot-film probe technique can be employed in a three-dimensional flowfield.

### Acknowledgment

This research was conducted under the McDonnell Douglas Independent Research and Development program.

### References

- <sup>1</sup>Roos, F. W., "Hot-Film Probe Technique for Monitoring Shock-Wave Oscillations," *Journal of Aircraft*, Vol. 16, Dec. 1979, pp. 871-875.
- <sup>2</sup>Sajben, M. and Crites, R. C., "Real-Time Optical Measurements of Time-Dependent Shock Position," *AIAA Journal*, Vol. 17, Aug. 1979, pp. 910-912.
- <sup>3</sup>Roos, F. W., "Some Features of the Unsteady Pressure Field in Transonic Airfoil Buffeting," *Journal of Aircraft*, Vol. 17, Nov. 1980, pp. 781-788.
- <sup>4</sup>Sajben, M., Bogar, T. J., and Kroutil, J. C., "Forced Oscillation Experiments in Supercritical Diffuser Flows with Application to Ramjet Instabilities," AIAA Paper 81-1487, July 1981.

#### AIAA Journal

### AIAA Meetings of Interest to Journal Readers\*

Date	Meeting (Issue of <i>AIAA Bulletin</i> in which program will appear)	Location	Call for Papers†	Abstract Deadline
<b>1983</b>				
Jan. 10-13	<b>AIAA 21st Aerospace Sciences Meeting (Nov.)</b>	MGM Grand Hotel Reno, Nev.	April 82	July 6, 81
April 12-14	<b>AIAA 8th Aeroacoustics Conference</b>	Terrace Garden Inn Atlanta, Ga.	June 82	Aug. 31, 82
May 10-12	<b>AIAA/ASME/ASCE/AHS 24th Structures, Structural Dynamics &amp; Materials Conference</b>	Sahara Hotel Lake Tahoe, Nev.		
May 10-12	<b>AIAA Annual Meeting and Technical Display</b>	Long Beach Convention Center Long Beach, Calif.		
June 1-3	<b>AIAA 18th Thermophysics Conference (Apr.)</b>	The Queen Elizabeth Hotel, Montreal, Quebec, Canada		
June 27-29	<b>AIAA/SAE/ASME 19th Joint Propulsion Conference (Apr.)</b>	Westin Hotel Seattle, Wash.		
July 12-14	<b>16th Fluid and Plasma Dynamics Conference</b>	Radisson Ferncroft Hotel and Country Club, Danvers, Mass.		

\*For a complete listing of AIAA meetings, see the current issue of the *AIAA Bulletin*.

†Issue of *AIAA Bulletin* in which Call for Papers appeared.

‡Cosponsored by AIAA. For program information, write to: AIAA Meetings Department, 1290 Avenue of the Americas, New York, N.Y. 10104.